Millennial-scale storminess variability in the northeastern United States during the Holocene epoch

Anders J. Noren*, Paul R. Bierman*, Eric J. Steig†, Andrea Lini* & John Southon‡§

* *Department of Geology, University of Vermont, Burlington, Vermont 05405, USA*
† *Quaternary Research Center and Department of Earth and Space Sciences, University of Washington, Seattle, Washington 98195, USA*
‡ *Center for Accelerator Mass Spectrometry, Lawrence Livermore National Laboratory, Livermore, California 94551, USA*

For the purpose of detecting the effects of human activities on climate change, it is important to document natural change in past climate[1]. In this context, it has proved particularly difficult to study the variability in the occurrence of extreme climate events, such as storms with exceptional rainfall[1]. Previous investigations have established storm chronologies using sediment cores from single lakes[2–8], but such studies can be susceptible to local environmental bias. Here we date terrigenous inwash layers in cores from 13 lakes, which show that the frequency of storm-related floods in the northeastern United States has varied in regular cycles during the past 13,000 years (13 kyr), with a characteristic period of about 3 kyr. Our data show four peaks in storminess during the past 14 kyr, approximately 2.6, 5.8, 9.1 and 11.9 kyr ago. This pattern is consistent with long-term changes in the average sign of the Arctic Oscillation[9], suggesting that modulation of this dominant atmospheric mode may account for a significant fraction of Holocene climate variability in North America and Europe.

Lakes in the hilly terrain of Vermont and eastern New York contain sedimentary archives that consist of organic lake mud (gyttja), punctuated by layers of terrestrially derived material[2]. These terrigenous layers are commonly coarser, less organic, and contain more macrofossils of terrestrial plants than the surrounding gyttja; they are graded[2] and have distinctive stable isotopic signatures[3]. Previous work has demonstrated that such terrigenous layers are deposited by exceptional runoff events when rainfall of great intensity and/or duration affects mountainous lake drainage basins[2–8]. In New England, the heaviest rains occur during localized convective storms, "nor'easters" or other mid-latitude cyclones, and (more rarely) tropical storms, hurricanes, or their remnants. During and immediately after these events, material stored in upland streams and on steep basin hillslopes is eroded and transported to lake basins—as indicated by our field observations during two major storms, during which we documented increased fluvial transport of woody forest debris, sand and gravel into lakes. Thus, stratigraphic analysis and dating of lake sediment cores allows the determination of palaeostorm chronologies[2–8].

Other mechanisms (earthquakes, fires, lake-level fluctuations, and removal of vegetation by drought or disease) may also cause or facilitate the deposition of terrigenous material in lakes, but the effects of such other forcings have been shown to be minimal in New England[2,3]. The first European settlers in the area deforested most of the landscape, but the significant effects of these and other human activities are limited to the past ~250 yr (ref. 3). Snowmelt floods do not transport enough sediment to cause the deposition of terrigenous layers[5,8]. Analyses of cores from lakes with small, low-relief drainage basins show that periods of low aquatic primary productivity have not occurred in this region during the Holocene[3].

§ Present address: Earth System Science, University of California, Irvine, California 92697-3100, USA

Analyses of nine alluvial fans near our coring sites show periods of aggradation caused by increased storminess, runoff and hillslope erosion[3,10] correlated in time with the lacustrine storm records we present here. Most relevant to the argument that terrigenous layers in lake sediment represent storms are findings in locations with long documentary records, which reveal a strong correlation between heavy rainfall and the occurrence and thickness of terrigenous layers in lacustrine sediment[4–7].

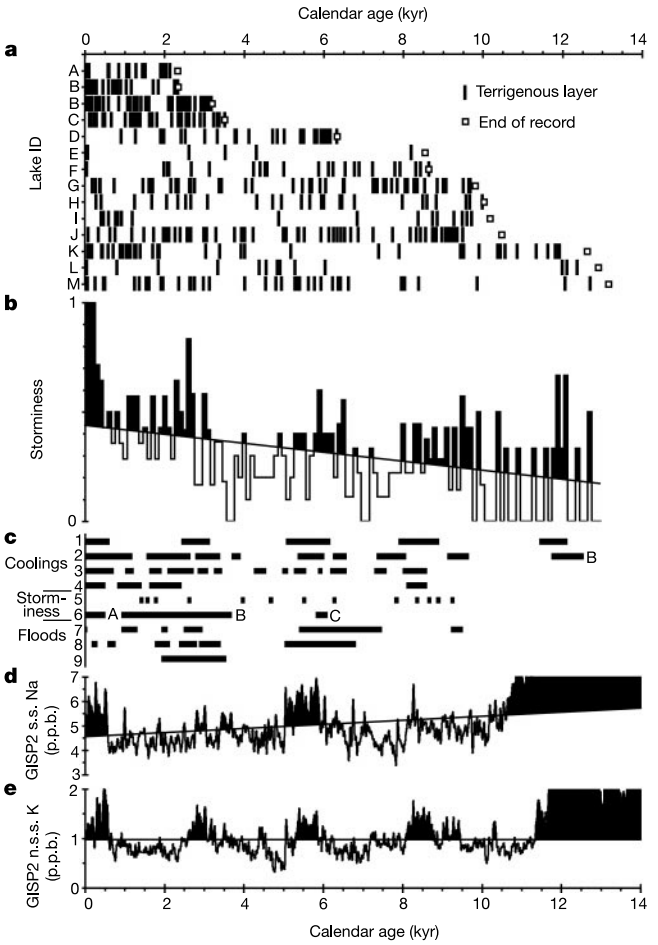

Figure 1 Inferred storminess in the northeastern United States and relevant climate records. **a**, Individual terrigenous sedimentation event chronologies from study lakes. Letters correspond to lakes in Supplementary Information map and table. Replicate cores recovered in each of four basins contained similar stratigraphies. Two cores were recovered from one lake, each in a distinct depocentre. These depocentres record terrigenous sediment delivery from different stream basins. **b**, Histogram of terrigenous sedimentation events (100-yr bins). Values above the superimposed linear regression are shaded. Histogram values are weighted by the inverse of the number of chronologies that cover each time interval. The trend in the data may reflect the slow progradation (growth) of the stream deltas into the lakes, toward the coring locations. As these deltas approach, smaller pulses of sediment are more readily transported to the coring locations. **c**, Other relevant climate records. Coolings as follows. 1, GISP2 glaciochemical cold events[21]. 2, Glacial expansions in the Alps[23]; 2B, the Younger-Dryas event[15]. 3, Glacial expansions in Scandinavia[24,25]. 4, Norwegian glacial expansions[26]. 5, Storm-related aggradational events on alluvial fans in Vermont[3,10]. Storminess as follows. 6A, LIA historical evidence[18]; 6B, high frequency of hurricane landfalls along the northern Gulf of Mexico coast[19]; 6C, occurrence of storm surge deposits on the northwestern coast of England[20]. Floods as follows. 7, Increased magnitude of 1.58-yr recurrence interval floods in the north-central United States (NCUS)[17]. 8, Increased magnitude of the largest floods in the NCUS[17]. 9, Highest frequency of megafloods on the Mississippi River[16]. **d**, GISP2 sea-salt (s.s.) Na and **e**, GISP2 non-sea-salt (n.s.s.) K concentrations, with values above the superimposed linear regressions shaded[21]. Other GISP2 aerosol deposition time series[21] exhibit variability similar to s.s. Na and n.s.s. K

We cored 13 small lakes with steep surrounding hillslopes, deep water, steep perimeter bathymetry, and inflowing streams with sandy deltas. The lakes were geographically distributed across a 20,000-km^2 region in Vermont and eastern New York (Supplementary Information). We used a percussion corer fitted with a piston to recover sediment cores from locations in deep water, adjacent to the stream delta foreslopes. The cores vary in length from 3.5 to 6 m, spanning 2.1 to 13.2 kyr (Fig. 1a).

We documented core stratigraphy with visual logging, magnetic susceptibility measurements, high-resolution X-radiography and loss-on-ignition[2]. We created a composite record for each core from the results of these four primary analyses. The composite record overcomes the limitations of the individual analyses, and most accurately represents the locations and thickness of terrigenous layers. Comparison of our composite record with the results from high-resolution, whole-core grain size analysis[11,12], a more sensitive analysis for determining the locations of terrigenous deposits, shows good agreement, and indicates that the composite record emphasizes the most extreme sediment delivery events (Fig. 2, and Supplementary Information).

We dated the cores with 80 accelerator mass spectrometer (AMS) ^{14}C ages of single terrestrial plant macrofossils and calibrated these dates using CALIB v4.2 (ref. 13; see also Supplementary Information). To account for the difference in sedimentation rates between the rapidly deposited terrigenous layers[3] and the slow accumulation of gyttja, we excluded the terrigenous layers from each record before creating age models, and assumed constant sedimentation rates between successive radiocarbon ages[2]. Combining the age models with the composite sediment records yields a dated event record for each lake (Fig. 1a, and Supplementary Information). Using the 14 event chronologies, we created a single histogram indicating the frequency of depositional events and by inference, the most severe storms during the Holocene (Fig. 1b).

The results presented here emphasize the importance of using the sediment from multiple lakes for this type of palaeoclimate reconstruction. Storm records derived from individual lake basins[2] vary owing to several factors, including the geologic character of the drainage basin, local differences in antecedent soil moisture or other factors of landscape conditioning[7], and core location. Such records may not reveal clear relationships between local events and wider climate patterns. Aggregate data derived from multiple sources are less susceptible to local environmental variability, and reveal regional landscape response to large-scale climate variability on long timescales.

The delivery of terrigenous sediment to the 13 lakes reached broad and variable maxima lasting ~1,500 yr, with the highest peaks centred at approximately 2.6, 5.8, 9.1 and 11.9 kyr before present (BP). Before European settlement of the area at ~250 yr BP, when deforestation and livestock grazing accelerated rates of hillslope erosion (which overprints our record[3]), sediment delivery appears to have been increasing toward another peak. This most recent period of increased delivery began at about 600 yr BP, coincident with the beginning of the Little Ice Age (LIA)[14]; the earliest such period peaked during the Younger Dryas climate interval[15].

Other, independent records of storminess and flooding from around the North Atlantic show maxima that correspond to those that characterize our lake records[16–20] (Fig. 1c). For example, oscillations in Holocene glaciochemical records from central Greenland ice cores are similar to storminess records in New England lakes. In particular, the time series of sea-salt sodium (s.s. Na) in the Greenland Ice Sheet Project Two (GISP2) core, believed to be an indicator of storminess and sea spray in the atmosphere of the high-

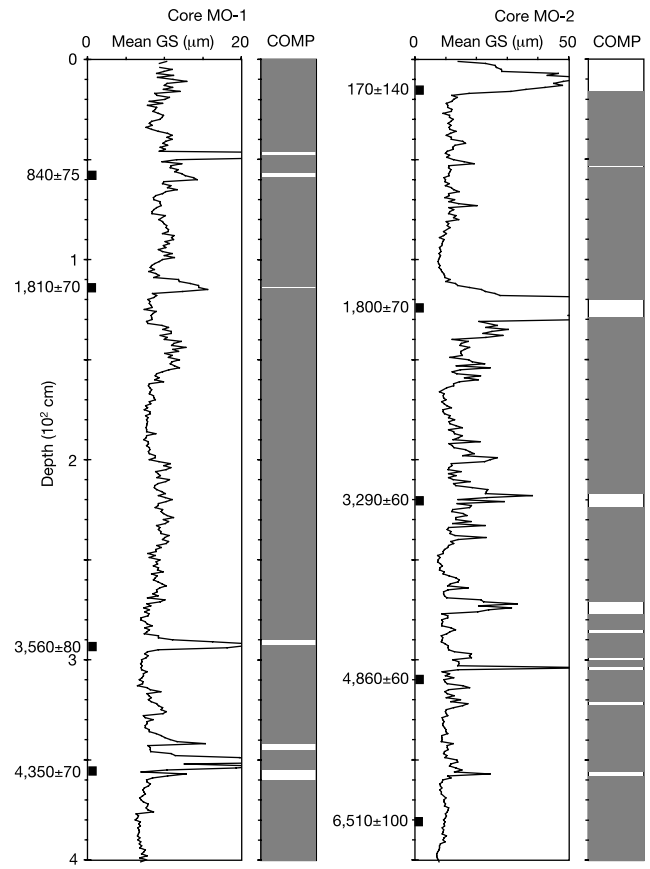

Figure 2 Results of high-resolution, whole-core grain size (GS) analysis and composite sediment record (COMP) for two Lake Morey cores. MO-1 is the distal core and MO-2 is the proximal core. Peaks in GS reflect high-energy fluvial transport events and thus the location of terrigenous layers (indicated in composite sediment record with white bands). Calibrated ^{14}C dates (with 1σ uncertainties) shown for each core.

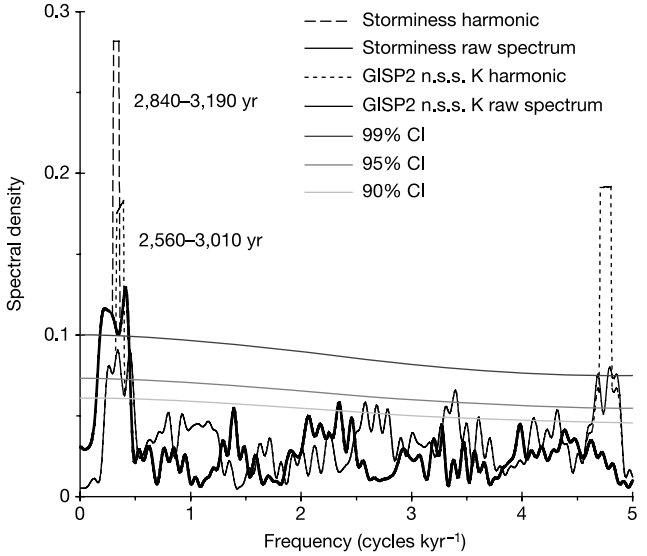

Figure 3 Multitaper spectral analysis (three tapers) of storminess and GISP2 non-sea-salt (n.s.s) K time series, interpolated with a 100-yr interval and with linear trend removed[29]. Spectral analysis of other GISP2 aerosol deposition time series[21] reveal power spectra similar to that of n.s.s. K. The harmonic spectrum represents the estimated significant periodic component of the raw spectrum, as measured by the Thomson variance ratio test for periodic signals (*F*-test). CI, confidence interval. Confidence levels are relative to red noise estimated from lag-1 autocorrelation with a median averaging filter[30]. The n.s.s. K raw spectrum has been rescaled such that the confidence intervals apply to both power spectra.

latitude North Atlantic region[21,22], exhibits peaks at times similar to the maxima identified here (Fig. 1d). Other GISP2 aerosol deposition time series (notably non-sea-salt potassium, n.s.s. K) show a similar pattern (Fig. 1e). Thus, the frequency of storm-related floods in the northeastern United States appears to be related to widespread North Atlantic climate variability on millennial timescales. Lacustrine data thus support the interpretation of the GISP2 glaciochemical record in terms of large-scale atmospheric circulation changes[15].

The pacing of storminess maxima derived from the various North Atlantic palaeoclimate records suggest a quasi-periodic cycle of ~3,000 yr (refs 16–21). Spectral analysis of our New England storminess time series (Fig. 3) reveals significant spectral power in a broad, double peak centred at a period of ~3,070 yr. A similar double peak exists in the power spectrum of the GISP2 time series of aerosol deposition[21] (Figs 1d, e and 3). Monte Carlo simulations ($n = 1{,}000$) show that the likelihood of obtaining comparable results from a composite of arbitrary lake sediment records (produced by randomly rearranging the events identified in each individual time series) is less than 1%.

The pacing of maxima and the power spectra of the New England lake-core and Greenland ice-core time series are remarkably similar, suggesting control of both by large-scale atmospheric circulation patterns. Annually resolved Na concentrations in ice cores from North Greenland[22] show a significant correlation with the characteristic patterns of sea level pressure associated with the Arctic Oscillation (AO)[9] during the past four decades. If, as argued by O'Brien and others[21], enhanced aerosol deposition to the Greenland ice sheet on longer timescales similarly reflects an increase in the relative strength of meridional versus zonal circulation, then increased New England storminess would coincide with a mode of atmospheric circulation most similar to the low phase of the contemporary AO, when high-latitude westerlies are weakened[9]. Conversely, times when New England storm frequency was low would coincide with the enhanced zonal flow of the high-phase AO.

Indeed, such a relationship between New England storminess and the AO has recently been confirmed for modern climate conditions by Thompson and Wallace[9], who show that nor'easters are four times as likely to occur during low-phase than during high-phase AO. Thus, millennial-scale variability in New England storminess may reflect modulation of the preferred phase of the AO on millennial timescales. This explanation is appealing, because it makes a specific prediction that New England storminess should be at its greatest when Europe is cold (characteristic of the low-phase AO). Comparison of our results with the other climate records (Fig. 1), including European glacier fluctuations, suggests that, as predicted, intense storms in New England tend to occur more frequently during periods that are cooler than average in Europe[15,21,23–26].

Atmospheric modes, such as the AO and El Niño/Southern Oscillation (ENSO), account for significant fractions of modern climate variability on interannual timescales[1,9]. In contrast to other researchers' conclusions[27], our results suggest that such dominant atmospheric modes may be modulated on longer timescales, and may therefore account for much of the variability in the palaeoclimate record. Changes in the AO, perhaps modulated by solar forcing[28], may explain a significant portion of Holocene climate variability in the North Atlantic region.

Climate models suggest that human activities, specifically the emission of atmospheric greenhouse gases, may lead to increases in the frequency of severe storms in certain regions of the Northern Hemisphere[1]. However, the existence of natural variability in storminess confounds reliable detection of anthropogenic effects. During the past ~600 yr, New England storminess appears to have been increasing naturally (Fig. 1b). This rhythm in storm frequency may explain some of the recently observed increases in extreme precipitation events[1]. If the pattern of millennial-scale variability that we documented through the Holocene persists into the future, New England storminess would continue to increase for the next ~900 yr. Because climate synopses compiled from instrumental records cannot distinguish underlying natural increases in storminess from anthropogenic effects, detected increases in contemporary storminess may not be a reliable indicator of human-induced climate change. □

Methods

Layer identification

We identified significant terrigenous layers in time series by comparing peaks to the background signal. To establish appropriate background estimates, we used singular spectrum analysis (lags = 20) to identify the first principal component in each series, after setting all data points greater than 1σ from the median to equal the median. Any shifts in the original data series that were more than 1σ from the first principal component were considered to be significant. Hence, significance is conservatively measured relative to the local background, rather than the entire data series.

In the composite sediment record, most terrigenous layers were identified when two or more of the individual analytical techniques detected such layers. In some cases, layers were identified from the results of a single analysis. The composite record is similar to records produced by the individual laboratory analyses, and all resulting storminess histograms produced from these individual analyses show similar millennial-scale pacing and yield similar power spectra. We find no correlation between sediment accumulation rates and the frequency of inferred storm events ($r^2 = 0.05$).

Obtaining layer data

Our laboratory 1-cm core sampling interval produced median temporal core sampling intervals ranging from 2 yr in lakes with the highest sedimentation rates, to 27 yr in lakes with the lowest sedimentation rates, and the interval varied throughout each core owing to the effects of autocompaction and changing sedimentation rates. We used several different interpolation intervals (varying from 10 to 200 yr) to obtain evenly spaced data for spectral analysis, all of which produced similar results. The results are robust to varying resolutions and tapers, and comparable results were obtained with the multitaper, Blackman–Tukey, and maximum entropy methods, as well as periodogram analysis using the Lomb–Scargle method (which avoids the need to interpolate the data).

Testing for variability

In addition to spectral analysis, we tested our storminess time series for statistically significant variability using several other methods. First, we examined the effect of removing individual time series from our aggregate record and again performing the spectral analyses. We find that in all cases, removal of an individual record retains the spectral peak at ~3,000 yr, though in some cases with confidence levels reduced to 95% relative to red noise. Second, we created 13 new time series by rearranging the data from each according to a random uniform distribution. In this way, we created time series with the same number of events but with those events randomly distributed in time. In all cases, we find that changing one time series maintains the spectral peak at ~3,000 yr, though again in some cases with confidence levels reduced to <95% relative to red noise. If we replace two or more of the original time series with the random time series, the identified spectral peak is reduced in each case to significantly lower confidence (<90%). Third, our Monte Carlo approach tested the likelihood of obtaining a significant (at 95%) spectral peak between 2,600 and 3,400 yr using the multitaper method and 13 random time series produced as described above. Using 1,000 attempts yields a <0.005 probability of obtaining such a peak in this interval.

Received 10 June; accepted 12 September 2002; doi:10.1038/nature01132.

1. Houghton, J. T., Ding, Y. & Griggs, D. J. (ed.) *Climate Change 2001: The Scientific Basis* (Cambridge Univ. Press, Cambridge, 2001).
2. Brown, S. L., Bierman, P. R., Lini, A. & Southon, J. R. 10,000 yr record of extreme hydrologic events. *Geology* **28,** 335–338 (2000).
3. Bierman, P. R. *et al.* Postglacial ponds and alluvial fans: Recorders of Holocene landscape history. *GSA Today* **7,** 1–8 (1997).
4. Eden, D. N. & Page, M. J. Palaeoclimatic implications of a storm erosion record from late Holocene lake sediments, North Island, New Zealand. *Palaeogeogr. Palaeoclimatol. Palaeoecol.* **139,** 37–58 (1998).
5. Lamoureux, S. F. Five centuries of interannual sediment yield and rainfall-induced erosion in the Canadian High Arctic recorded in lacustrine varves. *Wat. Resour. Res.* **36,** 309–318 (2000).
6. Nesje, A., Dahl, S. O., Matthews, J. A. & Berrisford, M. S. A ~4500-yr record of river floods obtained from a sediment core in Lake Atnsjøen, eastern Norway. *J. Paleolimnol.* **25,** 329–342 (2001).
7. Rodbell, D. T. *et al.* An ~15,000-year record of El Niño-driven alluviation in southwestern Ecuador. *Science* **283,** 516–520 (1999).
8. Thorndycraft, V., Hu, Y., Oldfield, F., Crooks, P. R. J. & Appleby, P. G. Individual flood events detected in the recent sediments of the Petit Lac d'Annecy, eastern France. *Holocene* **8,** 741–746 (1998).
9. Thompson, D. W. J. & Wallace, J. M. Regional climate impacts of the northern hemisphere annular mode. *Science* **293,** 85–89 (2001).
10. Jennings, K. L., Bierman, P. R. & Southon, J. R. Timing and style of deposition on humid-temperate fans, Vermont, USA. *Geol. Soc. Am. Bull.* (in the press).
11. Bosley, A. C., Bierman, P. R., Noren, A. J. & Galster, J. C. Identification of paleoclimatic cycles during the Holocene using grain size analysis of sediments cored from Lake Morey in Fairlee, VT. *Geol. Soc. Am. Abstr. Prog.* **33,** 15 (2001).
12. Conlan, A. *Vermont Geological Society Spring Meeting* (Norwich Univ., Norwich, VT, 2001).

13. Stuiver, M. & Reimer, P. J. Extended ^{14}C data base and revised CALIB 3.0 ^{14}C age calibration program. *Radiocarbon* **35,** 215–230 (1993).
14. Grove, J. M. *The Little Ice Age* (Methuen, London, 1988).
15. Mayewski, P. A. *et al.* Changes in atmospheric circulation and ocean ice cover over the North Atlantic during the last 41,000 years. *Science* **263,** 1747–1751 (1994).
16. Brown, P., Kennett, J. P. & Ingram, B. L. Marine evidence for episodic Holocene megafloods in North America and the northern Gulf of Mexico. *Paleoceanography* **14,** 498–510 (1999).
17. Knox, J. C. Sensitivity of modern and Holocene floods to climate change. *Quat. Sci. Rev.* **19,** 439–457 (1999).
18. Lamb, H. H. Variation and changes in the wind and ocean circulation: the Little Ice Age in the northeast Atlantic. *Quat. Res.* **11,** 1–20 (1979).
19. Liu, K. b. & Fearn, M. L. Reconstruction of prehistoric landfall frequencies of catastrophic hurricanes in northwestern Florida from lake sediment records. *Quat. Res.* **54,** 238–245 (2000).
20. Zong, Y. & Tooley, M. J. Evidence of mid-Holocene storm-surge deposits from Morecambe Bay, northwest England: A biostratigraphical approach. *Quat. Int.* **55,** 43–50 (1999).
21. O'Brien, S. R. *et al.* Complexity of Holocene climate as reconstructed from a Greenland ice core. *Science* **270,** 1962–1964 (1995).
22. Fischer, H. Imprint of large-scale atmospheric transport patterns on sea-salt records in northern Greenland ice cores. *J. Geophys. Res.* **106,** 23977–23984 (2001).
23. Hormes, A., Müller, B. U. & Schlüchter, C. The Alps with little ice: evidence for eight Holocene phases of reduced glacier extent in the Central Swiss Alps. *Holocene* **11,** 255–265 (2001).
24. Karlén, W. & Kuylenstierna, J. On solar forcing of Holocene climate: evidence from Scandinavia. *Holocene* **6,** 359–365 (1996).
25. Boulton, G. S., *et al. Glacier Fluctuations during the Holocene* (eds Frenzel, B., Boulton, G. S., Gläser, B. & Huckriede, U.) 5–23 (Fischer, Stuttgart, 1997).
26. Matthews, J. A., Dahl, S. O., Nesje, A., Berrisford, M. & Andersson, C. Holocene glacier variations in central Jotunheimen, southern Norway based on distal glaciolacustrine sediment cores. *Quat. Sci. Rev.* **19,** 1625–1647 (2000).
27. Bond, G. *et al.* Persistent solar Influence on North Atlantic climate during the Holocene. *Science* **294,** 2130–2136 (2001).
28. Shindell, D. T., Schmidt, G. A., Mann, M. E., Rind, D. & Waple, A. Solar forcing of regional climate change during the Maunder minimum. *Science* **294,** 2149–2152 (2001).
29. Thomson, D. J. Spectrum estimation and harmonic analysis. *Proc. IEEE* **70,** 1055–1096 (1982).
30. Mann, M. E. & Lees, J. M. Robust estimation of background noise and signal detection in climatic time series. *Clim. Change* **33,** 409–445 (1996).

Supplementary Information accompanies the paper on *Nature*'s website (**http://www.nature.com/nature**).

Acknowledgements We thank J. Galster for field and laboratory assistance, K. Jennings for field assistance, A. Bosley and A. Conlan for grain size analysis, S. Brown for laboratory training, P.T. Davis for coring device design and training, and J. M. Wallace and H. Fischer for comments and discussion. This work was supported by the US National Science Foundation (P.R.B).

Competing interests statement The authors declare that they have no competing financial interests.

Correspondence and requests for materials should be addressed to A.J.N. (e-mail: anders.noren@alumni.carleton.edu).

The strength of $Mg_{0.9}Fe_{0.1}SiO_3$ perovskite at high pressure and temperature

Jiuhua Chen, Donald J. Weidner & Michael T. Vaughan

Mineral Physics Institute and Department of Geosciences, State University of New York at Stony Brook, Stony Brook, New York 11794-2100, USA

The Earth's lower mantle consists mainly of $(Mg,Fe)SiO_3$ perovskite and (Mg,Fe)O magnesiowüstite, with the perovskite taking up at least 70 per cent of the total volume[1]. Although the rheology of olivine, the dominant upper-mantle mineral, has been extensively studied, knowledge about the rheological behaviour of perovskite is limited. Seismological studies indicate that slabs of subducting oceanic lithosphere are often deflected horizontally at the perovskite-forming depth, and changes in the Earth's shape and gravity field during glacial rebound indicate that viscosity increases in the lower part of the mantle. The rheological properties of the perovskite may be important in governing these phenomena. But $(Mg,Fe)SiO_3$ perovskite is not stable at high temperatures under ambient pressure, and therefore mechanical tests on $(Mg,Fe)SiO_3$ perovskite are difficult. Most rheological studies of perovskite have been performed on analogous materials[2–7], and the experimental data on $(Mg,Fe)SiO_3$ perovskite are limited to strength measurements at room temperature in a diamond-anvil cell[8] and microhardness tests at ambient conditions[9]. Here we report results of strength and stress relaxation measurements of $(Mg_{0.9}Fe_{0.1})SiO_3$ perovskite at high pressure and temperature. Compared with the transition-zone mineral ringwoodite[10] at the same pressure and temperature, we found that perovskite is weaker at room temperature, which is consistent with a previous diamond-anvil-cell experiment[8], but that perovskite is stronger than ringwoodite at high temperature.

The perovskite sample was synthesized at 26 GPa and 2,100 K from a glass of composition $(Mg_{0.9}Fe_{0.1})SiO_3$. X-ray diffraction confirmed the pure perovskite phase. *In situ* stress measurements were performed using a large-volume press (SAM85) at the X17B beamline of the National Synchrotron Light Source[11]. Stress in the sample was measured by monitoring the broadening of diffraction peaks from the sample at high pressure and temperature. The experiment is described briefly below; details of the methodology, along with previous studies on mantle-related materials, can be found elsewhere[10,12,13].

The synthesized sample was powdered at liquid-nitrogen temperature to prevent amorphization, and loaded into a high-pressure cell together with a layer of NaCl as an internal pressure calibrant. The experiment was conducted by first increasing the pressure to 20 GPa, and then increasing the temperature. At each temperature, energy-dispersive X-ray diffraction patterns were collected as a function of time to characterize the stress relaxation. The sample pressure was monitored by comparing the compression of NaCl to the Decker scale[14], and the sample temperature was measured by a $W_{97}Re_3$–$W_{75}Re_{25}$ thermocouple. In all the X-ray diffraction patterns from the sample at the pressures and temperatures reported here, no back transformation was observed. When temperature was later increased above 1,273 K, the diffraction pattern showed a back transformation in the sample because the experiment was carried out at a pressure lower than the perovskite stability field. Our stress measurements are therefore limited to the data collected up to 1,073 K.

Heterogeneous deviatoric stress at each grain of the powdered sample, together with very small grain sizes, gives rise to diffraction

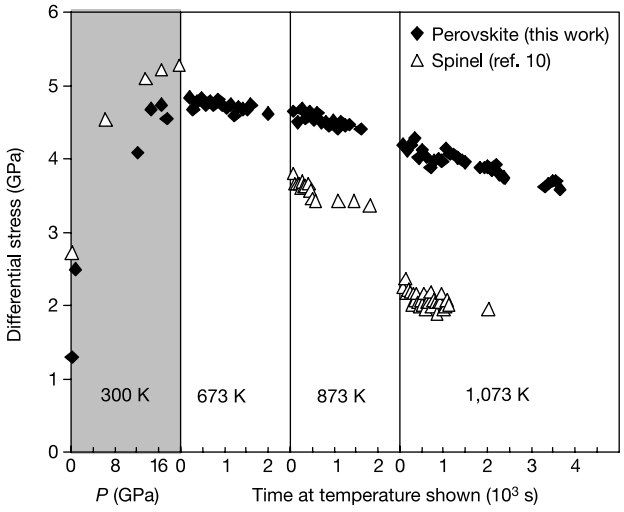

Figure 1 Differential stress supported by $Mg_{0.9}Fe_{0.1}SiO_3$ perovskite and Mg_2SiO_4 spinel as a function of time at several constant temperatures under ~20-GPa confining pressure. Filled diamonds, perovskite (this work); open triangles, spinel (from previous study[10]). Data in the shaded area correspond to stresses of the sample during loading.

